

Novel Self-Sustained Modulation in Superconducting Stripline Resonators

Eran Segev, Balaegh Abdo, Oleg Shtempluk, and Eyal Buks

Microelectronics Research Center, Department of
Electrical Engineering, Technion, Haifa 32000, Israel

Nonlinear effects in superconductors are important for both basic science and technology. A strong nonlinearity may be exploited to demonstrate some important quantum phenomena in the microwave region, such as quantum squeezing^{1,2,3} and experimental observation of the so called dynamical Casimir effect⁴; Whereas technologically, these effects may allow some intriguing applications such as bifurcation amplifiers for quantum measurements^{5,6} and resonant readout of qubits⁷. In this work we study the response of a superconducting (SC) microwave stripline resonator to a monochromatic injected signal. We find that there is a certain range of driving parameters, in which a novel nonlinear phenomenon emerges, and self-sustained modulation (SM) of the reflected power of the resonator is generated by the resonator. That is, the resonator undergoes limited cycle oscillations, ranging between several to tens of megahertz. A theoretical model which attributes the SM to a thermal instability yields a good agreement with the experimental results. A similar phenomenon was briefly reported in the 60's^{8,9,10,11} in dielectric resonators which were partially coated by a SC film, but it was not thoroughly investigated and therefore its significance was somewhat overlooked. This phenomenon is of a significant importance as it introduces an extreme nonlinear mechanism, which is by far stronger than any other nonlinearity observed before in SC resonators¹². It results in high intermodulation gain, substantial noise squeezing, period doubling of various orders¹², and strong coupling between resonance modes (see supplementary figure 1).

Our device (Fig. 1 (b) – (d)) integrates a narrow microbridge into a SC stripline ring resonator. The impedance of the microbridge strongly affects the normal modes of the resonator and thus the resonance frequencies can be tuned by either internal (Joule selfheating) or external (infrared illumination¹³) perturbations¹⁴. Further design considerations, fabrication details as well as normal modes calculation can be found elsewhere¹³. The experiments are performed using the setup described in Fig. 1 (a). We stimulate the resonator with a monochromatic tone at an angular frequency ω_p , and measure the reflected power of the resonator by a spectrum analyzer in the frequency domain and an oscilloscope in the time domain. Measurements are carried out while the device is fully immersed in liquid Helium.

Fig. 2, panels (a) and (b) show typical experimental results of the SM phenomenon in the

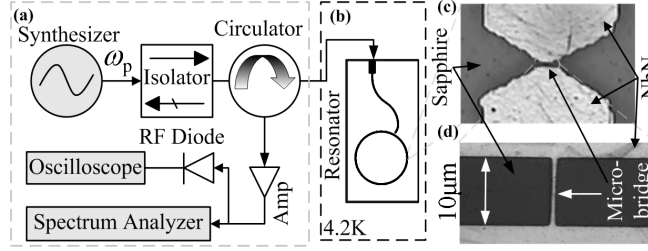


FIG .1: (a) SM measurement setup. (b) Schematic layout of the device. The resonator is designed as a stripline ring, having a characteristic impedance of 50Ω . It is composed of 200nm thick NbN deposited on a Sapphire wafer. A weakly coupled feedline is employed for delivering the input and output signals. An optical microscope image of the ring resonator section at which the microbridge is integrated is seen in panel (c), whereas panel (d) shows the microbridge, whose dimensions are $1 \times 10 \mu\text{m}^2$.

frequency domain. The resonator is stimulated with a monochromatic tone at the resonance frequency of the third mode f_3 , and the dependence of the SM on the injected pump power is investigated. At relatively low and relatively high input power ranges ($P_{\text{pump}} \in [33.25 \text{ dBm}, 23.7 \text{ dBm}]$) the response of the resonator is linear, namely, the reflected power of the resonator contains a single spectral component at the frequency of the stimulating pump tone ω_p . In between these power ranges, regular SM of the reflected power of the resonator occurs (see panel (b), subplots (ii;iv)). It is realized by rather strong and sharp sidebands, which extend over several hundred megahertz at both sides of the resonance frequency. The SM frequency, which is defined as the frequency difference between the pump and the primary sideband, increases as the pump power increases. The regular SM starts and ends at two power thresholds, referred to as the lower and the upper power thresholds. The lower power threshold (panel (b), i) spreads over a very narrow power range of approximately 10 nW, during which the resonator experiences a strong amplification of the noise floor (noise rise) over a rather large frequency band, especially around the resonance frequency itself. This noise rise can be explained in terms of nonlinear dynamics theory, as it predicts the occurrence of strong noise amplification near a threshold of instability^{16,17}. The upper power threshold (panel (b), vi) spreads over a slightly larger power range than the lower one and has similar, but less extreme characteristics.

The SM nonlinearity is also strongly dependent on the pump frequency. This dependence

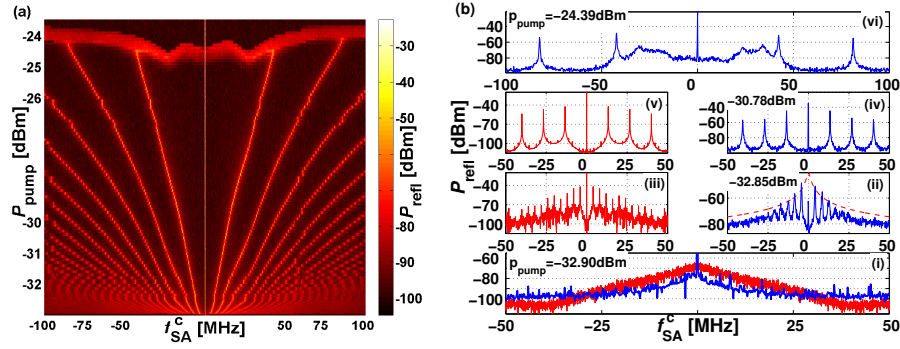


FIG. 2: Typical experimental results of the SM phenomenon in the frequency domain. Panel (a) plots a color map of the reflected power P_{refl} as a function of the pump power P_{pump} and the measured frequency f_{SA} , centralized on the pump frequency, which coincides with the resonance frequency $f_3 = 5.74 \text{ GHz}$ ($f_{\text{SA}}^c = f_{\text{SA}} = f_3$). Panel (b), subplots (i); (ii); (iv); (vi), plot the same measurement at four different pump powers, corresponding to (i) the lower power threshold, (ii) and (iv) powers that are in the range of regular SM, and (vi) the upper power threshold. The red curve in subplot (ii), which has a Lorentzian shape, shows the spectral density of the SM sidebands as predicted theoretically by the model (Eq. 26 of Ref.¹⁵). The solid red curve in subplot (i) was obtained by numerically integrating the equations of motion of the model with a nonvanishing noise at the first power threshold and evaluating the spectral density¹⁵. Subplots (iii) and (v) were obtained by numerically integrating the equations of motion of the model for the noiseless case, at input powers corresponding to subplots (ii) and (iv) respectively, and calculating the spectral density.

is shown in the supplementary video 1, where each frame is a graph similar to Fig. 2, panel(a), and corresponds to a different pump frequency, starting at a red shifted pump frequency ($f = f_{\text{pump}} - f_3 < 0$) and ending at a blue shifted pump frequency ($f = f_{\text{pump}} - f_3 > 0$). Fig. 3 plots the SM frequency as a function of the pump frequency and power. The inset plots the stability diagram of the resonator (to be discussed below) as a function of the same parameters. The SM occurs only within a well-defined frequency range around the resonance frequency. A small change in the pump frequency can abruptly ignite or quench the SM. Once started though, the modulation frequency has a weak dependence on the

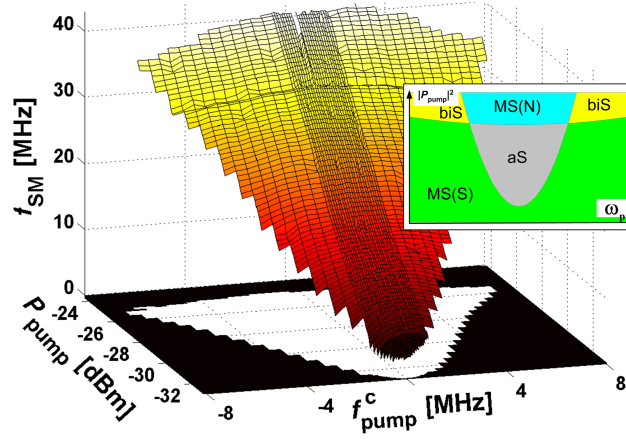


FIG. 3: SM frequency f_{SM} as a function of the pump power and the pump frequency, centralized on the resonance frequency $f_{pump}^C = f_{pump} - f_3$. The inset shows a schematic diagram of the stability zones of the resonator as a function of the pump power and frequency. The green, pale blue, yellow, and grey colors represent the SC monostable (MS(S)), NC monostable (MS(N)), bistable (biS), and astable (aS) zones respectively.

pump frequency. The maximum SM frequency measured with this device is approximately 41 MHz, whereas higher maximum of approximately 57 MHz has been measured with other devices¹⁵.

We propose a theoretical model according to which the SM originates from a thermal instability in the microbridge section of the SC stripline resonator. Current-carrying superconductors are known to have two or more metastable phases sustained by Joule self-heating¹⁸. One is the SC phase and the other is an electrothermal local phase, known as hotspot, which is basically an island of normal conducting (NC) domain, with a temperature above the critical one, surrounded by a SC domain. This phenomenon can be explained by the heat balance equation holding at more than one temperature. A perturbation can trigger or suppress the formation of a hotspot and thus the microbridge can oscillate between instable phases. Such oscillations were often observed in experiments, for the case of a SC microbridge driven by an external dc voltage (see review¹⁸ and references therein).

In the current case, as the microbridge is integrated into a stripline resonator, the system is driven into instability via externally injected microwave pump tone. We herein briefly present the corresponding theoretical model, whereas the full derivation of the equations, as

well as experimental justifications to several assumptions are included elsewhere¹⁵. Consider a resonator driven by a weakly coupled feedline carrying an incident coherent tone $b^{\text{in}} e^{i\omega_p t}$, where b^{in} is constant complex amplitude ($b^{\text{in}^2} / P_{\text{pump}}$) and ω_p is the driving angular frequency. The mode amplitude inside the resonator can be written as $B e^{i\omega_p t}$, where $B(t)$ is a complex amplitude which is assumed to vary slowly on a time scale of $1/\omega_p$. In this approximation, the equation of motion of B reads².

$$\frac{dB}{dt} = [i(\omega_p - \omega_0) - \gamma] B - \frac{P}{i\omega_p} b^{\text{in}} + c^{\text{in}}; \quad (1)$$

where $\omega_0(T)$ is the temperature dependant angular resonance frequency, T is the temperature of the hotspot, $\gamma = \gamma_1 + \gamma_2$, where γ_1 is the coupling constant between the resonator and the feedline, and $\gamma_2(T)$ is the temperature dependant damping rate of the mode. The term c^{in} represents an input Gaussian noise with a zero-mean and a random phase. We consider a case where the nonlinearity originates by a local hotspot in the microbridge. If the hotspot is assumed to be sufficiently small, its temperature T can be considered as homogeneous. The temperature of other parts of the resonator is assumed to be equal to that of the coolant T_0 . The power Q heating up the hotspot is given by $Q = Q_t$ where $Q_t = \frac{1}{2} \omega_0^2 \beta J^2$ is the total power dissipated in the resonator, and $0.6 \leq \beta \leq 1$ represents the portion of the dissipated power that is being absorbed by the microbridge. The heat balance equation reads

$$C \frac{dT}{dt} = Q - W; \quad (2)$$

where C is the thermal heat capacity, $W = H(T - T_0)$ is the heat transfer power to the coolant, and H is the heat transfer coefficient.

Nonlinearity, according to our simple theoretical model, results by coupling the equation of motion of the mode amplitude in the resonator, Eq. (1), to the thermal balance equation in the microbridge, Eq. (2). The coupling mechanism is based on the dependence of both the resonance frequency ω_0 and the damping rate γ_2 of the driven mode on the resistance of the microbridge¹⁴, which in turn depends on the temperature of the microbridge. We assume the simplest case, where this dependence is a step function that occurs at the critical temperature T_c . We further assume that all other parameters are temperature independent. In our previous publication¹³ we have thoroughly investigated the dependence of the resonance modes on the resistance of the microbridge. We have shown that a resonance frequency can be smoothly shifted by gradually controlling the bridge resistance. In addition the damping

rate increases up to a certain maximum, as the resistance increases, but then decreases back to approximately its original value, when the resistance is further increased.

Due to the step-like dependence of the resistance, and the dependence of the heat generation, on the temperature of the microbridge¹⁸, the system may have in general up to two locally stable steady states, corresponding to the SC and NC phases. These states are associated with stationary solutions of the uncoupled Eq. (1) and (2), where the noise is disregarded. The stability of each of these phases depends on both the power and frequency parameters of the injected pump tone. In general there exist four different stability zones (see inset in Fig 3)¹⁵. Two are monostable zones, where either the SC phase or the NC phase is locally stable. Another is a bistable zone, where both phases are locally stable^{19,20}. The third is an astable zone, where none of the phases are locally stable, and consequently the resonator is expected to oscillate between the two phases. As the two phases significantly differ in their reflection coefficients, the oscillations translate into a modulation of the reflected pump tone. The mechanism introduced in this theoretical model is somewhat similar to one of the mechanisms which cause self oscillations in an optical parametric oscillator²¹.

The dependence of the SM on the input power, as observed in the time domain (Fig. 4), gives a complementary understanding of the SM phenomenon. Below the lower power threshold the resonator is in the SC low reflective phase, where only a small portion of the injected power is reflected off the resonator. Once the pump power approaches the power threshold, sporadic spikes in the reflected pump power occur, as seen in subplot (i). Near the threshold the device is in sub-critical conditions and these spikes are caused by a stochastic noise which triggers transitions of the microbridge from the SC phase to the NC high reflective phase. During a transition the stored energy in the resonator is quickly discharged and dissipated. Consequently, after a quick and short warm-up the microbridge cools down until eventually it switches back to the SC phase. As a result, the damping rate decreases back to its original value and thus the stored energy in the resonator is slowly built up again. Once a spike is triggered, the noise has a negligible effect on the dynamics of the energy discharge and buildup and therefore the line-shapes of the various spikes are similar. This behavior can also be clearly observed in the simulation results, shown in subplot (v).

Regular SM of the reflected power (Fig. 4 (ii;vi)) occurs when the pump power is set above the lower power threshold. In this case the pump tone drives the resonator to the astable state and the noise has a negligible influence. The dynamics of the oscillations is

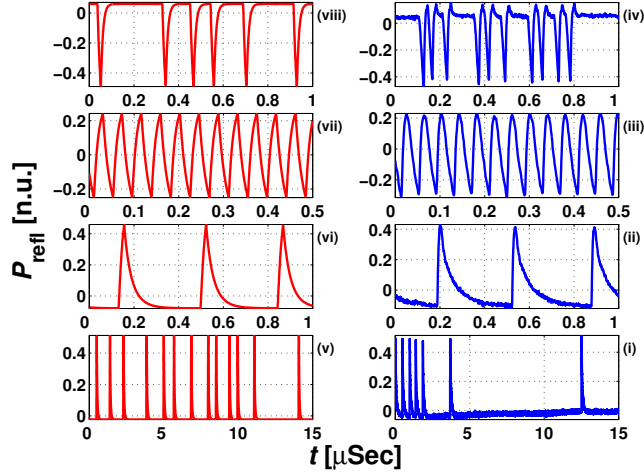


FIG. 4: Panels (i) – (iv) show typical experimental results of the SM phenomenon in the time domain. The reflected power is normalized by the value of the maximum peak to peak amplitude. AC coupling is employed in the measurement and thus a zero value represents the average measured power. Each panel refers to a different pump power range, (i) lower power threshold, (ii) and (iii) powers corresponding to regular SM, (iv) upper power threshold. Panels (v) – (viii) show numerical integration of Eqs. (1) and (2) calculated for the above-mentioned four cases. The graphs are centralized around their mean value and normalized by the value of the maximum peak to peak amplitude. In the simulation of the lower and upper thresholds (panels (v) and (viii)), a Gaussian thermal noise, corresponding to 4.2 K and 15 K temperatures was assumed respectively, whereas in the simulation of the regular SM, (panels (vi) and (vii)), the noise was disregarded. Supplementary video 2 shows the SM in the time domain while gradually increasing the pump power from frame to frame. Each frame has a subplot similar to panels (i) – (iv), and a subplot similar to 2(b) panels (ii), (iv).

similar to the one just described where the energy buildup time is strongly dependant on the pump power. Thus, the oscillation frequency is faster for higher pump power values (Fig. 4 (iii;vii)). The upper power threshold (Fig. 4 (vi)) resembles the lower one, but the SC and NC phases exchange roles. The resonator is in the NC high reactive phase, and noise-induced spikes temporarily drive it to the SC low reactive phase. The internal thermal noise in the upper threshold is stronger than in the lower one and consequently this power threshold range is wider.

In conclusion, we report on a novel nonlinear phenomenon where SM is generated in a SC microwave stripline resonator. This behavior is robust and occurs in all of our devices and at various resonance frequencies. A theoretical model according to which the SM originates by a thermal instability is introduced. In spite of its simplicity, the model exhibits a good quantitative agreement with the experimental results. In our measurements we find strong and correlated nonlinear phenomena accompanying the SM¹². One of these phenomena is self-excitation (SE) of coupled resonance modes, which is shortly described in a supplementary figure. This phenomenon may be exploited for state readout in quantum data processing systems³.

Acknowledgements We thank Bernard Yurke, Ron Lifshitz, Mike Cross, Oded Gottlieb, and Steven Shaw for valuable discussions. This work was supported by the German Israel Foundation, the Israel Science Foundation, the Deborah Foundation, the Poznanski Foundation, and MAFAT.

Author Information Reprints and permissions information is available at npg.nature.com/reprintsandpermissions. The authors declare no competing financial interests. Correspondence and requests for materials should be addressed to S.E.~(email: segeve@tx.technion.ac.il).

-
- ¹ Movshovich, R. et al. Observation of zero-point noise squeezing via a josephson-parametric amplifier. *Phys. Rev. Lett.* 65, 1419{1422 (1990).
 - ² Yurke, B. & Buks, E. Performance of cavity-parametric amplifiers, employing kerr nonlinearities, in the presence of two-photon loss (2005). *ArXiv:quant-ph/0505018*.
 - ³ Buks, E. & Yurke, B. Dephasing due to intermode coupling in superconducting stripline resonators. *Phys. Rev. A* 73, 023815 (2005).
 - ⁴ Arbel-Segev, E., Abdo, B., Shtempluck, O. & Buks, E. Towards experimental study of the dynamical casimir effect (2006). *ArXiv:quant-ph/0606099*.
 - ⁵ Siddiqi, I. et al. Dispersive measurements of superconducting qubit coherence with a fast latching readout. *Phys. Rev. B* 73, 054510 (2006).
 - ⁶ Wiesenfeld, K. & McNamara, B. Small-signal amplification in bifurcating dynamical systems. *Phys. Rev. A* 33, 629{642 (1986).

- ⁷ Lee, J. C., Oliver, W. D., Berggren, K. K. & Orlando, T. P. Nonlinear resonant behavior of the dispersive readout scheme for a superconducting qubit (2006). URL <http://www.citebase.org/abstract?id=oai:arXiv.org:cond-mat/0609561>.
- ⁸ Clorfeine, A. S. Nonlinear reactance and frequency conversion in superconducting films at millimeter wavelengths. *Appl. Phys. Lett.* 4, 131 (1964).
- ⁹ D'Aiello, R. V. & Freedman, S. J. Parametric amplification and oscillations in structured superconducting tin films. *Appl. Phys. Lett.* 9, 323 (1966).
- ¹⁰ Peskovatskii, S. A., Era, I. I. & Barilovich, O. I. Nonlinear properties of a superconducting lead film at microwave frequencies. *JETP Lett* 6, 227 (1967).
- ¹¹ Enu, I. I., Kashchei, V. A. & Peskovatskii, S. A. Thin superconducting films in a UHF-field II. nonlinear properties of thin superconducting films in a UHF field. *Sov. Phys. JETP* 31, 416 (1970).
- ¹² Arbel-Segev, E., Abdo, B., Shtempluck, O. & Buks, E. Extreme nonlinear phenomena in NbN superconducting stripline resonators (2006). *ArXiv: cond-mat/0607262*.
- ¹³ Arbel-Segev, E., Abdo, B., Shtempluck, O. & Buks, E. Fast resonance frequency optical modulation in superconducting stripline resonator. *IEEE Trans. Appl. Superconduct.* 16, 1943 (2006).
- ¹⁴ Saeedkia, D., Majidi, A. H., Safavi-Naeini, S. & Mansour, R. R. Frequency and time-varying scattering parameters of a photo-excited superconducting microbridge. *IEEE Microwave Wireless Compon. Lett.* 15, 510{512 (2005).
- ¹⁵ Arbel-Segev, E., Abdo, B., Shtempluck, O. & Buks, E. Thermal instability and self-sustained modulation in superconducting NbN stripline resonators (2006). *ArXiv: cond-mat/0607261*.
- ¹⁶ Wiesenfeld, K. Noisy precursors of nonlinear instabilities. *J. Stat. Phys.* 38, 1071 (1985).
- ¹⁷ Kravtsov, Y. A., Bilchinskaya, S. G., Butkovskii, O. Y., Rychka, I. A. & Surovyatkina, E. D. Bifurcational noise rise in nonlinear systems. *JETP* 93, 1323 (2001). *Zh. Eksp. Teor. Fiz.* 120, pp. 1527 (2001).
- ¹⁸ Gurevich, A. V. & Mints, R. G. Self-heating in normal metals and superconductors. *Rev. Mod. Phys.* 59, 941{999 (1987).
- ¹⁹ Abdo, B., Segev, E., Shtempluck, O. & Buks, E. Observation of bifurcations and hysteresis in nonlinear NbN superconducting microwave resonators. *IEEE Trans. Appl. Superconduct.* 16, 1976 { 1987 (2006).
- ²⁰ Abdo, B., Segev, E., Shtempluck, O. & Buks, E. Nonlinear dynamics in the resonance line

shape of NbN superconducting resonators. Phys. Rev. B 73, 134513 (2006).

- ²¹ Suret, P., Derozier, D., Lefranc, M., Zemmouri, J. & Bielawski, S. Self-pulsing instabilities in an optical parametric oscillator: Experimental observation and modeling of the mechanism. Phys. Rev. A 61, 021805 (2000).